Neutron scattering investigation of the static critical properties of Rb_2CrCl_4

1993 J. Phys.: Condens. Matter 5 7871

(http://iopscience.iop.org/0953-8984/5/42/009)

J. Phys.: Condens. Matter 5 (1993) 7871–7892. Printed in the UK

Neutron scattering investigation of the static critical properties of Rb_2CrCl_4

J Als-Nielsen†¶, S T Bramwell‡, M T Hutchings§, G J McIntyre‡ and D Visser‖

† Risø National Laboratory, DK-4000 Roskilde, Denmark
‡ Institut Max von Laue–Paul Langevin, 156X, 38042 Grenoble Cédex, France
§ Non-Destructive Testing Department, AEA Industrial Technology, Harwell Laboratory, Didcot OX11 0RA, UK
‖ Department of Physics, Loughborough University of Technology, Leicestershire LE11 3TU, UK

Received 5 January 1993, in final form 7 July 1993

Abstract. We have investigated the static zero-field critical properties of the ionic ferromagnet Rb_2CrCl_4, using neutron scattering, under conditions such that the quasi-static approximation is valid. A general consideration of the spin Hamiltonian of Rb_2CrCl_4, with $S = 2$, shows that it approximates the two-dimensional (2D) XY model, with additional weak perturbations. Rb_2CrCl_4 orders three dimensionally at $T_C = 52.3$ K, and very close to T_C there is a regime of three-dimensional critical behaviour. However, both below and above T_C there is a crossover to regimes of two-dimensional critical fluctuations. In these regimes, there is excellent agreement between experiment and theoretical predictions for a finite-sized 2D XY model, suggesting that Rb_2CrCl_4 is an ideal realization of this system.

1. Introduction

In this paper we report the results of an investigation of the static zero-field critical properties of dirubidium chromous chloride (Rb_2CrCl_4), using neutron scattering techniques. Rb_2CrCl_4 is a rare example of an insulating compound which orders ferromagnetically at $T_C \simeq 52$ K. In terms of its critical properties, the results presented here show that it can be regarded as an experimental realization of the two-dimensional (2D) XY model.

The ferromagnetism of Rb_2CrCl_4 is strongly 2D in character on account of its crystal structure, in space group $Cmca$ [1]. This is a co-operative Jahn–Teller distorted superstructure of that of K_2NiF_4, itself with the space group $I4/mmm$, in which the magnetic Cr^{2+} $3d^4$ ions are arranged in planar square arrays with very weak coupling to adjacent layers (figure 1(a)). The ferromagnetic sign of the dominant superexchange between the nearest-neighbour Cr^{2+} ions arises from the nature of their coupling via the chloride ions. These Cl^- ions are moved slightly off the mid-Cr^{2+} positions, so that the D_{2h} environment of the Cr^{2+} ions approximates to an elongated octahedron of Cl^- ions with the long axis alternating by 90° from one Cr^{2+} ion to its neighbour. With this axis as the z axis, the three t_{2g} orbitals and the e_g $(3z^2 - r^2)$ orbitals of Cr^{2+} are occupied by one electron each, and the e_g $(x^2 - y^2)$ orbital is empty. The orbital moment of the Cr^{2+} ion is quenched, but the D_{2h} crystal field with spin–orbit coupling gives rise to two single-ion anisotropy

¶ Present address: European Synchrotron Radiation Facility, 156X-38042 Grenoble, France.

0953-8984/93/427871+22$07.50

terms which, together with the isotropic exchange interaction, act in the spin Hamiltonian on the $S = 2$ spin states. The larger planar anisotropy term confines the spins to lie in the planes [2], while the weaker uniaxial term favours the alignment of alternate spins at 90°. The resultant of the exchange field (favouring parallel alignment) and the in-plane uniaxial anisotropy term is a slight canting of the ordered spins below T_C by approximately $\pm 1°$ from the ⟨110⟩ direction [1, 3]. We shall, throughout this paper, refer directions to the reciprocal lattice of the related K_2NiF_4 unit cell, which has lattice constants $a_0 = 5.90$ Å and $c_0 = 15.75$ Å at 50 K.

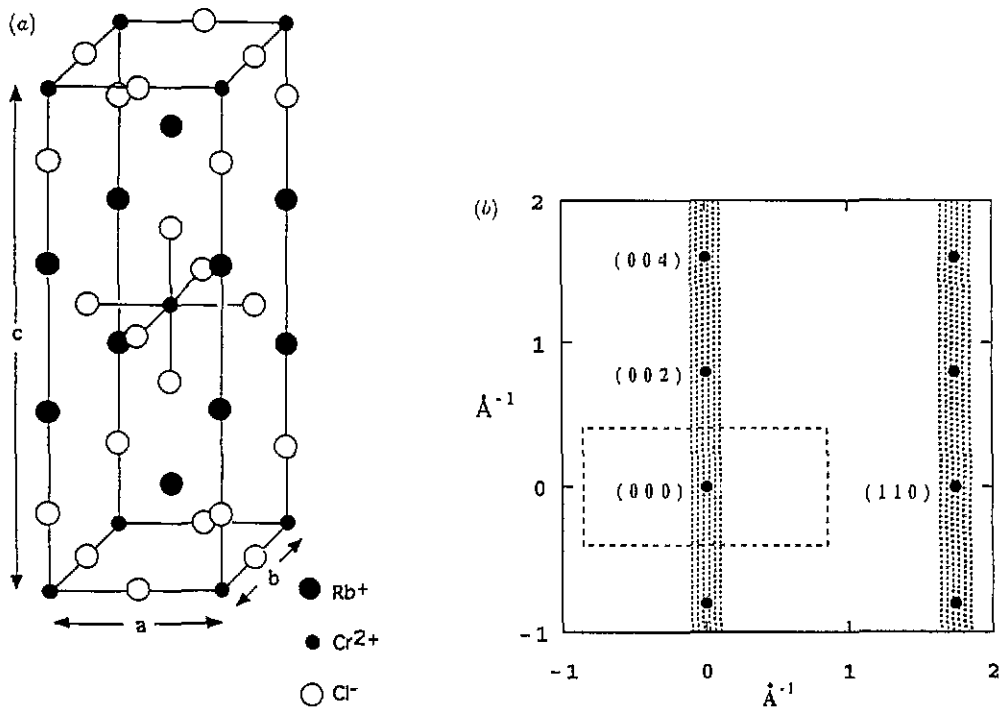

Figure 1. (*a*) Approximate crystal structure of Rb_2CrCl_4, represented in the $I4/mmm$ space group. The true crystal structure is a Jahn–Teller distorted superstructure of that shown, in which the bridging halogen atoms move slightly off the mid-Cr^{2+} positions. (*b*) Section in the $(1, -1, 0)$ plane of the reciprocal lattice of Rb_2CrCl_4 ($I4/mmm$) corresponding to the scattering plane of the present experiment: ●, reciprocal-lattice points; - - - -, boundary of the first Brillouin zone; the shaded areas indicate the rods of critical scattering.

The consequence of the presence of several terms in the spin Hamiltonian of differing magnitudes is to give rise to a sequence of crossover behaviour in the critical properties of Rb_2CrCl_4, between different 'universality classes'. According to the universality hypothesis (see, e.g., [4]), in magnets with short-range interactions, the critical behaviour depends upon only two parameters: the lattice dimensionality D and the spin dimensionality d. In Rb_2CrCl_4, the major interaction is that of the nearest-neighbour Heisenberg exchange, which cannot alone give long-range order in two dimensions in an infinite system [5], and the next largest is the single-ion anisotropy which confines the spins to the plane. So first Heisenberg ($D = 2$; $d = 3$) and then XY-like ($D = 2$; $d = 2$) behaviour might be expected to dominate as T_C is approached. However, the uniaxial term and small interplanar exchange will become important very close to T_C.

Of particular interest is the possible 2D XY-like behaviour of Rb_2CrCl_4. The 2D Heisenberg model is known to be particularly sensitive to planar anisotropy [6], and so in the absence of other perturbations one would expect XY critical behaviour of the 'Kosterlitz–Thouless' (KT) type, with no long-range order, but rather a phase transition involving the unbinding of spin vortices [7, 8]. In fact the small in-plane anisotropy and interplanar coupling cause a phase transition to long-range order, but some of the properties of the KT transition appear to survive. Cornelius *et al* [9] analysed the bulk magnetization of Rb_2CrCl_4 according to the predictions of unmodified KT theory and found good agreement. Recently it has been argued [10] that real compounds approximating 2D behaviour with planar anisotropy, of which Rb_2CrCl_4 is probably the best example, may be considered to be equivalent to ideal 2D XY systems of finite size. Well above T_C, these should approximate pure 2D XY behaviour but, below T_C, finite-size effects should become dominant. The finite 2D XY system is predicted [10] to have a spontaneous magnetization below T_C, and a distinct universal critical behaviour characterized by a magnetization exponent $\beta = 0.23$. These theoretical predictions are briefly summarized in section 3. One of the results of the present experimental work will be confirmation of these predictions.

In the next two sections the spin Hamiltonian for Rb_2CrCl_4 will be given in detail, and the expected critical behaviour of the 2D XY model will be discussed. In section 4, details of the neutron scattering experiments and methods of data analysis will be given. The results are presented in section 5 and discussed in section 6. Conclusions are drawn in section 7.

2. Hamiltonian

The spin Hamiltonian for Rb_2CrCl_4 has been discussed by Hutchings *et al* [3] and Harrop [11] (see also Elliott *et al* [12]). In writing the Hamiltonian the true orthorhombic symmetry of the structure may be neglected, since each layer itself has tetragonal symmetry and the coupling between the layers is very weak. We can then write

$$\hat{H} = \hat{H}_{ex} + \hat{H}_{anis} + \hat{H}_{dip} \tag{1}$$

where $\hat{H}_{ex}$ is the exchange term, $\hat{H}_{anis}$ is a single-ion anisotropy term and $\hat{H}_{dip}$ is the dipolar interaction. The dipolar term is relatively small because of the open structure and symmetry of the sites. The exchange term is given by

$$\hat{H}_{ex} = -J \sum_{ij}^{NN} \boldsymbol{S}_{i1} \cdot \boldsymbol{S}_{j2} - J' \sum_{i'j'}^{3rd\ NN} \boldsymbol{S}_{i'} \cdot \boldsymbol{S}_{j'} \tag{2}$$

where J is the nearest-neighbour (NN) Heisenberg exchange interaction between NN $S = 2$ spins in the (0, 0, 1) plane, and J' is the exchange constant between the third-NN spins, which lie in adjacent planes. The summations are taken over all spins i, j in the two sublattices 1, 2. Hutchings *et al* [3, 13] found $J/k_B = 7.56 \pm 0.19$ K, $J'/k_B = 0.0018 \pm 0.0004$ K, by fitting to the spin-wave energy dispersion at 20 K.

Defining the axes a, b and z, along the [1, 0, 0], [0, 1, 0] and [0, 0, 1] axes of the K_2NiF_4 cell, one has for the single-ion anisotropy

$$\hat{H}_{anis} = -\tilde{P} \sum_i (S_{i1a}^2 + S_{i2b}^2) + \tilde{D} \sum_i (S_{i1z}^2 + S_{i2z}^2) \tag{3}$$

where $\tilde{D}$ gives the planar anisotropy and $\tilde{P}$ the uniaxial term within the plane. Hutchings *et al* [3] found that $\tilde{D}/k_B = -0.41 \pm 0.17$ K and $\tilde{P}/k_B = 3.14 \pm 0.18$ K. If one neglects the canting of the spins of about 1.5°, one obtains the simpler expression

$$\hat{H}_{\text{anis}} = -P \sum_i S_{ix}^2 + D \sum_i S_{iz}^2 \tag{4}$$

where x now lies along the mean spin direction (110). In this case, $D/k_B = 1.06 \pm 0.15$ K and $P/k_B = 0.123 \pm 0.014$ K [3]. It should be noted that the difference between $\tilde{D}$ and D arises simply from the definition of the uniaxial terms. This may be seen by considering the more conventional form

$$\hat{H}_{\text{anis}} = -P' \sum_i (S_{ix}^2 - S_{iy}^2) + D' \sum_i S_{iz}^2 \tag{5}$$

where both terms now transform in the same way as combinations of spherical harmonics. By adding a constant term $\frac{1}{2}P(S_{ix}^2 + S_{iy}^2 + S_{iz}^2)$ to bring (4) into the form (5) it is seen that $D' = D + \frac{1}{2}P$ and $P' = \frac{1}{2}P$. Referring to (5), the term D' confines the spins to the x–y plane, and P' is a weak anisotropy within the plane. It is found that $D'/k_B = 1.12$ K, and $P'/k_B = 0.062$ K.

The more complete Hamiltonian (3) may be transformed in a similar way, by introducing the terms $\tilde{P}'$ and $\tilde{D}'$. In this case, it is found that $\tilde{D}'/k_B = 1.15$ K, and $\tilde{P}'/k_B = 1.57$ K. The uniaxial terms $\tilde{P}'$ and P' differ because they are referred to axes at 45°.

The staggered twofold anisotropy of Rb_2CrCl_4 approximates to an effective fourfold in-plane anisotropy field in the ordered phase of approximate magnitude $h_4 = P'S = 0.12$ K [11]. Thus Rb_2CrCl_4 may be regarded as a two-dimensional Heisenberg magnet with dominant planar anisotropy (about $0.15J$) and weaker fourfold anisotropy (about $0.015J$) and interlayer coupling (about $2.4 \times 10^{-4}J$).

3. 2D XY model

The 2D XY model cannot sustain long-range order in the thermodynamic limit, as was rigorously proved by Mermin and Wagner [5]. However, as originally shown by KT [7] and Berezinskii [8], the model does exhibit a phase transition to a low-temperature phase of infinite correlation length but no spontaneous order. This phase is characterized by a spin correlation exponent η defined such that, below the transition temperature T_{KT},

$$\langle S_0 \cdot S_r \rangle \sim r^{-\eta} \tag{6}$$

where the angular brackets represent the thermal average of the correlation between spins S separated by a distance r. The exponent η was predicted to increase with increasing temperature, reaching the universal value of 0.25 at T_{KT} [14].

In compounds approximating to 2D XY magnets, one would expect to observe pure model behaviour only in the paramagnetic regime above T_C, when the correlation length is sufficiently short that minor terms in the Hamiltonian are irrelevant. In this regime the 2D XY model has spin correlations which decay exponentially with a characteristic correlation length ξ (which we express in units of the lattice constant). Using renormalization group (RG) theory, Kosterlitz [14] predicted that the correlation length ξ diverges according to

$$\xi \simeq \exp[\pi/\sqrt{c(T - T_{KT})}] \tag{7}$$

where $c \simeq 2.1$ is a constant. Note that $\pi/\sqrt{c}$ has often been incorrectly written as approximately 1.5, following a trivial error in the original work; the correct value is approximately 2.2. The temperature in equation (7) is measured in units of the exchange constant. In terms of our present definition of J, which involves summation over all spins, the temperature is measured in units of $2JS^2$. In these units $T_{KT} = 1.35$ is the transition temperature of the so-called Villain [16] model, the particular approximation to the 2D XY model studied by Kosterlitz [14] and José *et al* [15]. In this approximation, the original cosine interaction between neighbouring spins is replaced by the quadratic term, but the periodicity of the cosine interaction is maintained in the partition function. Physically, this corresponds to a model containing only harmonic spin waves and vortices. The neglect of anharmonic terms is believed not to affect the critical behaviour, other than to renormalize T_{KT}. The value of $T_{KT} = 1.35$ for the Villain model, and the original mean-field estimate of KT [7] of about $\frac{1}{2}\pi(= 1.57)$ are both considerably higher than T_{KT} for the 2D XY model, of which the most accurate Monte Carlo estimate obtained by Gupta *et al* [17] is 0.898. In units of the exchange constant of Rb_2CrCl_4, these three estimates correspond to 82 K, 95 K and 55 K, respectively.

Gupta *et al* [17] determined the correlation length ξ of the 2D XY model from their numerical simulation and found excellent agreement with equation (7) over a wide temperature range above T_{KT}. However, because the transition temperature T_{KT} is in general a non-universal quantity it is more useful to rewrite equation (7) in terms of a dimensionless reduced temperature as follows:

$$\xi \simeq \exp[b/\sqrt{(T - T_{KT})/T_{KT}}] \tag{8}$$

where T_{KT} represents the actual KT transition temperature of a particular system. Equation (8) has the advantage that the amplitude b is dimensionless, which is not true of the constant c. The amplitude b, as defined above, is only weakly system dependent [18]. According to the corrected estimate of Kosterlitz, $b = \pi/\sqrt{cT_{KT}} \simeq 1.9$ and from the parameter b_ξ of Gupta *et al* [17] we find that $b \simeq 1.8$. These estimates are probably equal to within the accuracy to which b can be calculated.

In general in layered magnets the interlayer exchange induces both three-dimensional (3D) ordering and 3D critical behaviour. Below T_C, the correlation length rapidly decreases to a value ξ_{2D} where the interlayer exchange is irrelevant and 2D behaviour is again obtained. This crossover occurs at a temperature very close to T_C, and at lower temperatures the correlation length remains approximately constant. In this region the layered magnet may be considered to be equivalent to a 2D system of effective finite size L_{eff} given by

$$L_{eff} \simeq \xi_{2D} \simeq \sqrt{J/J'}. \tag{9}$$

In the case of the XY model, a finite-sized system can sustain a strong spontaneous magnetization, even though the infinite system cannot [19].

We now briefly describe the argument of Bramwell and Holdsworth [10], who considered a finite system of L^2 spins. The magnetization in the 2D regime is calculated through a spin-wave analysis, in which the effective spin-wave stiffness K_{eff} is renormalized by the presence of vortices:

$$M(T)/M(0) \simeq (1/L\sqrt{2})^{1/4\pi K_{eff}}. \tag{10}$$

The finite size is taken into account by using the system size L as the rescaling parameter in the renormalization group equations of José *et al* [15]. In the infinite system, at T_{KT}, K_{eff}

takes the universal value $2/\pi$ and as the temperature is increased jumps discontinuously to zero [20]. In the finite system the universal jump is rounded out, and K_{eff} decreases smoothly, reaching the value $2/\pi$ at a slightly higher temperature T^*:

$$(T^* - T_{\text{KT}})/T_{\text{KT}} = b^2/4(\ln L)^2. \tag{11}$$

This temperature is equivalent to T_{KT} in the infinite system, with the universal exponents $\eta = 1/2\pi K_{\text{eff}} = 0.25$, $\delta = 15$, and the magnetization (10) given by

$$M(T^*)/M(0) \simeq (1/L\sqrt{2})^{1/8}. \tag{12}$$

In general, T^* occurs quite far from the temperature at which the magnetization becomes close to zero. This temperature, T_{C}, may be defined as the temperature where the correlation length ξ, given by the Kosterlitz expression (7), becomes equal to the system size L. It is found that

$$(T_{\text{C}} - T_{\text{KT}})/T_{\text{KT}} = b^2/(\ln L)^2. \tag{13}$$

A critical exponent β may be defined with respect to T_{C} as follows:

$$\beta(L, T) = [\![\partial\{\ln[M(L, T)]\}/\partial\{\ln[T_{\text{C}}(L) - T]\}]\!]_L \tag{14}$$

which gives a remarkable universal result at T^*:

$$\beta(L, T^*) = 3\pi^2/128 = 0.231\ldots. \tag{15}$$

This power-law behaviour of the magnetization directly reflects the absence of the universal jump and the smooth decrease in K_{eff} in the finite system. In the thermodynamic limit, i.e. the limit $L \to \infty$, the behaviour passes continuously to that of KT theory. The magnetization then disappears as its amplitude becomes zero, through equation (10), but the result (15) remains valid until the limit.

The behaviour of layered XY magnets is obtained by substituting L by L_{eff} in the above equations. A wide variety of layered XY magnets do show $\beta = 0.23$ in the subcritical region, as observed for Rb_2CrCl_4 (e.g. K_2CuF_4 [21] and $Ba(NiPO_4)_2$ [22]). In these compounds, β is defined relative to the 3D ordering temperature T_{3D} rather than relative to the temperature T_{C} as defined above. This is understandable [10], since T_{C} and T_{3D} are both located in the temperature range where

$$\xi(\text{2D}\,XY) \sim \text{O}(\sqrt{J/J'}). \tag{16}$$

The rapid divergence of the 2D XY correlation length ξ (2D XY) ensures that this temperature range is very narrow, and so $T_{\text{C}} \simeq T_{\text{3D}}$. However, the fact that T_{C} and T_{3D} almost exactly coincide is perhaps surprising. We return to a discussion of this point in section 6, and in the meantime use 'T_{C}' to denote *both* the effective critical temperature defined in equation (13), and the 3D ordering temperature T_{3D}.

4. Experimental procedure

We have utilized the quasi-static approximation to magnetic neutron scattering, which is valid for sufficiently high incident neutron energies, or for certain scattering geometries [23,24]. Defining the scattering vector $\boldsymbol{Q} = \boldsymbol{k}_i - \boldsymbol{k}_f$ where $\boldsymbol{k}_i$ and $\boldsymbol{k}_f$ are the initial and final neutron wavevectors, the magnetic scattering function $S(\boldsymbol{Q})$ comprises both the Bragg scattering, which is proportional to the square of the spontaneous magnetization M, and the diffuse scattering, which is proportional to the product of the wavevector-dependent susceptibility $\chi(\boldsymbol{q})$ and the temperature T. Here $\boldsymbol{q}$ is defined as $\boldsymbol{q} = \boldsymbol{Q} - \boldsymbol{\tau}$, where $\boldsymbol{\tau}$ is the reciprocal-lattice vector of the magnetic structure. In general, scattering arises only from spin components perpendicular to the scattering vector $\boldsymbol{Q}$ and is weighted by the magnetic form factor. However, the latter varies slowly with $\boldsymbol{Q}$ and can often be neglected. The observed magnetic scattering as a function of $\boldsymbol{Q}$ is a convolution of $S(\boldsymbol{Q})$ with the instrumental resolution function. It has been found experimentally that $\chi(\boldsymbol{q})$ usually has a Lorentzian profile:

$$\chi(q) \simeq \chi(0)/[1 + (q/\kappa)^2] \tag{17}$$

where κ, the Lorentzian half-width at half-maximum, is equal to the inverse correlation length in the Ornstein–Zernike mean-field model [25].

The scattering from Rb_2CrCl_4 exhibits behaviour typical of quasi-2D magnets (see, e.g., Birgeneau *et al* [26]). The evolution of magnetic Bragg peaks reflects 3D ordering below T_C. The diffuse scattering on the other hand reflects the predominant 2D fluctuations, occurring as rods of intensity running parallel to the c direction in reciprocal space, intersecting the reciprocal-lattice points (figure 1(*b*)). Near to T_C, these rods have a maximum intensity at each Bragg point because of the effect of 3D exchange coupling. The evolution of the critical scattering is shown in figure 2. The intensity profile is approximately given by (17), with $\boldsymbol{q}$ in this case defined relative to a point on the $[0, 0, \zeta]$ rod (i.e. $\boldsymbol{\tau} = (0, 0, \zeta)$).

We report the results, some of which have already been referred to in previous publications [27], of two experiments on the similar samples, grown by Dr P J Walker at the Clarendon Laboratory, Oxford, using the Czochralski technique [28]. The first was performed in 1977 using the TAS6 spectrometer at Risø, and the second was performed in 1986 on the D10 spectrometer at the Institut Laue–Langevin (ILL), Grenoble. The experiments involved different instruments, personnel and methods of data analysis, and so a comparison of the results provides an unbiased check on systematic errors. The sample examined at Risø was roughly spherical in shape with a diameter of about 8 mm, and that used at the ILL was a roughly ellipsoidal single crystal of approximate dimensions 15 mm × 8 mm × 7 mm. In both experiments the sample was oriented with $[1, -1, 0]$ vertical, and so $[1, 1, 0]$ and $[0, 0, 1]$ lay in the scattering plane. The intensity of the $(0, 0, 4)$ Bragg reflection, which has a particularly weak nuclear component, and the $[0, 0, \zeta]$ diffuse rod were measured as a function of temperature and wavevector.

The TAS6 spectrometer at Risø was used in a two-axis mode with 30′ horizontal collimation before the pyrolitic graphite $(0, 0, 2)$ plane monochromator; 36′ horizontal and 27′ vertical collimation before the sample, and 28′ horizontal and 22′ vertical collimation before the ^{3}He detector. The neutrons of incident wavelength 2.45 Å passed through a pyrolitic graphite filter placed before the sample, to remove higher orders. The sample was mounted in a helium-filled aluminium can inside a Cryogenics Associates CT14 cryostat, and the temperature was measured using a platinum resistance thermometer. The resolution function for elastic scattering was carefully measured using the $(0, 0, 2)$ and $(0, 0, 4)$ Bragg

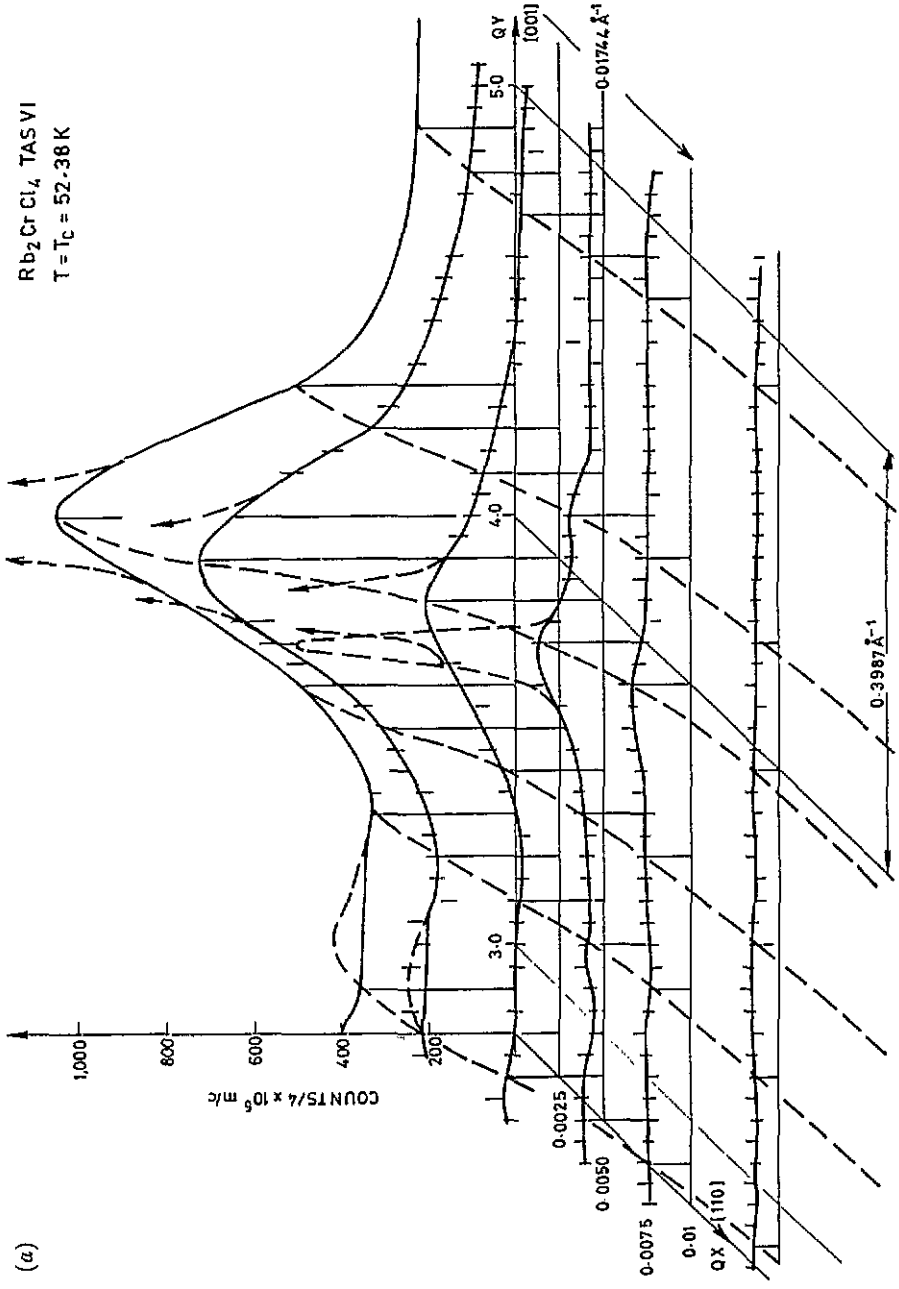

Figure 2. (a) Diffuse scattering of Rb_2CrCl_4 measured using the TAS6 spectrometer, near to the (0, 0, 4) reciprocal-lattice point at $T = 52.28$ K; ——, guide to the eye; ----, (0, 0, 4) Bragg reflection. The modulation of the critical scattering due to 3D effects is seen to commence below about 55 K.

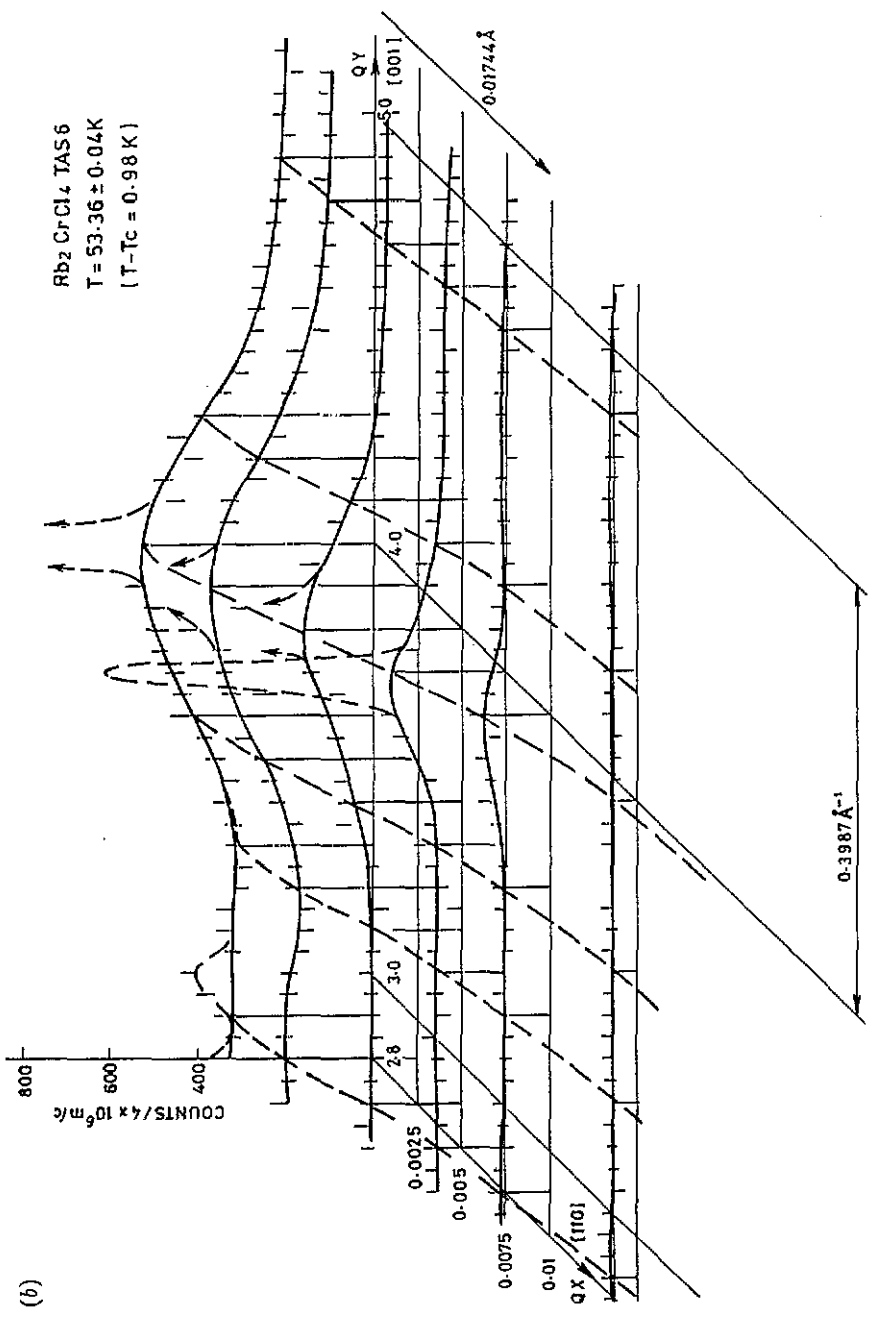

Figure 2. (b) Diffuse scattering of Rb_2CrCl_4 measured using the TAS6 spectrometer, near to the (0, 0, 4) reciprocal-lattice point at $T = 53.36$ K: ——, guide to the eye; - - - -, (0, 0, 4) Bragg reflection. The modulation of the critical scattering due to 3D effects is seen to commence below about 55 K.

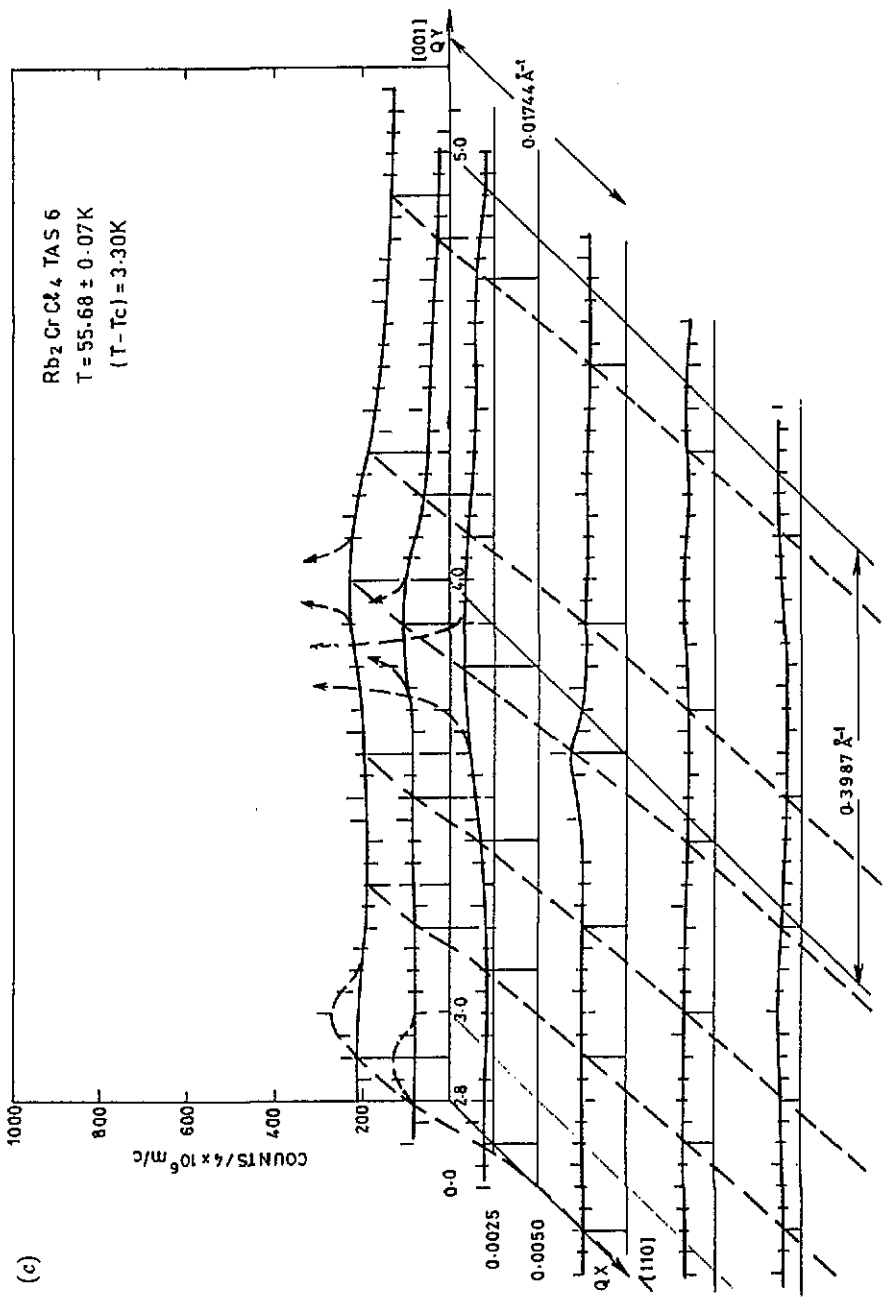

Figure 2. (c) Diffuse scattering of Rb_2CrCl_4 measured using the TAS6 spectrometer, near to the (0, 0, 4) reciprocal-lattice point at $T = 55.68$ K: ——, guide to the eye; - - - -, (0, 0, 4) Bragg reflection. The modulation of the critical scattering due to 3D effects is seen to commence below about 55 K.

reflections. It was used in the Harwell routine FITSQ [29] to analyse the data by convolving it in three dimensions with $S(Q)$, and fitting parameters in $S(Q)$ to the data using the Harwell routine VA02A; a typical fit is illustrated in figure 3(a). The magnetization was measured from the $(0, 0, 4)$ Bragg peak intensity, after carefully subtracting the diffuse critical scattering and nuclear scattering. T_C was estimated to be 52.403 ± 0.016 K. The diffuse scattering was measured at or near $Q = (0, 0, 2.9)$. Figure 2 shows certain scans in this region. By comparing data measured at $(1, 0, 2.9)$ and $(-1, 0, 2.9)$ it was confirmed that the width of the rod measured was independent of the geometry, and so the quasi-static approximation was good.

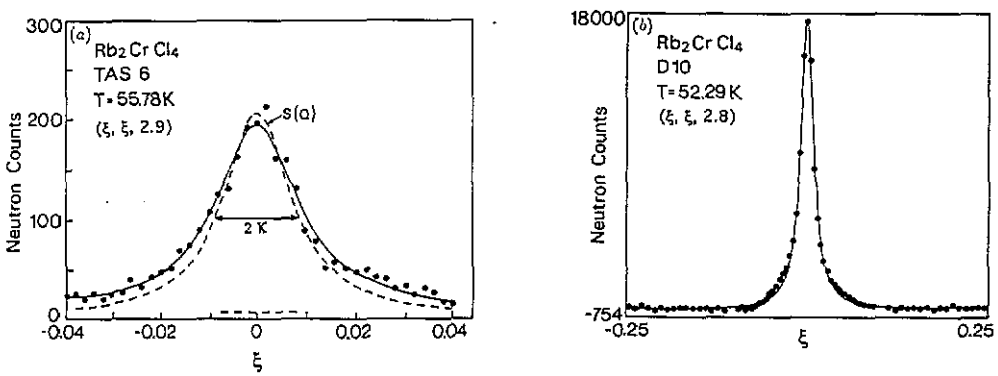

Figure 3. (a) Diffuse scattering of Rb_2CrCl_4 at 55.7 K near to $(0, 0, 2.9)$, measured using the TAS6 spectrometer: ——, fit to the data as described in the text; - - - -, scattering function $S(Q)$ before convolution with the instrumental resolution. (b) Diffuse scattering of Rb_2CrCl_4 at 52.29 K near to (0,0,2.8), measured using the D10 spectrometer, with a similar scan at 180 K subtracted: ——, fit to the data of a Lorentzian function convolved with a Gaussian function of width (HWHM) $0.0024 \times 2\pi/a_0$, to describe the instrumental resolution.

In the experiment performed using D10, the crystal was contained in a helium-filled can, mounted in an ILL 'Orange' cryostat, with the temperature measured with a platinum resistance thermometer. A neutron wavelength of 1.26 Å was used. The data were fitted using the one-dimensional fitting routine PKFIT to the Lorentzian function (17), which was convolved with a Gaussian function in order to describe the instrumental resolution. The resolution width (FWHM) was estimated by linear interpolation from the measured widths of the $(0, 0, 2)$ and $(0, 0, 4)$ Bragg reflections and varied between $0.48 \times 10^{-2} \times 2\pi/a_0$ Å^{-1} and $0.38 \times 10^{-2} \times 2\pi/a_0$ Å^{-1}, respectively. This method of correcting for instrumental resolution was not as rigorous as the method used for the TAS6 data but was expected to be satisfactory so long as the resolution width was an order of magnitude less than the observed width of the diffuse rod. The magnetization was again estimated from scans of the $(0, 0, 4)$ Bragg reflection, and T_C was found to be 52.225(5) K. The diffuse scattering was measured in scans of the wavevector perpendicular to $[0, 0, 1]$, centred on $(0, 0, \zeta)$, with ζ taking the values 2.2, 2.4, 2.6, 2.8 and 2.9. It was found that fits to the data were greatly facilitated by subtracting an identical scan measured at 180 K as a 'background', thereby removing the effect of any nuclear or other temperature-independent scattering. A typical fit to the data is illustrated in figure 3(b).

5. Results

5.1. Spontaneous magnetization

The relative spontaneous magnetization M was derived as the square root of the magnetic Bragg intensity and is shown in figure 4.

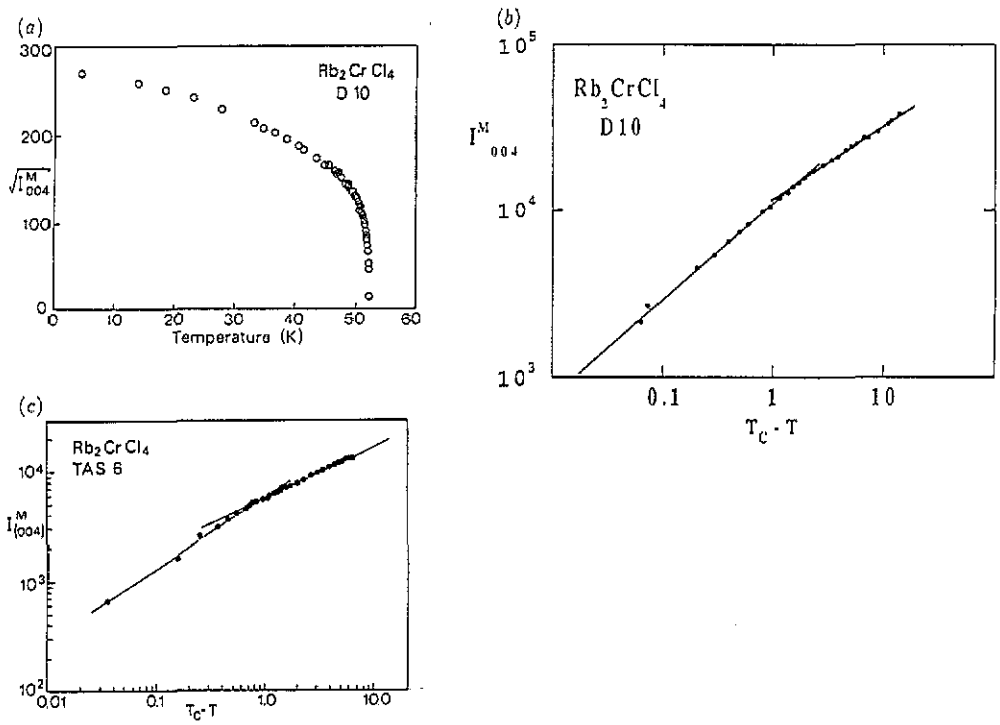

Figure 4. (*a*) Magnetization versus temperature for Rb_2CrCl_4, derived as the square root of the magnetic intensity of the (0, 0, 4) Bragg reflection, measured using the D10 spectrometer. (*b*), (*c*) The intensity of the (0, 0, 4) magnetic Bragg reflection plotted against the reduced temperature on logarithmic scales. The lines are of slope 2β, where the values of β determined are listed in table 1. The data clearly show two regimes of different β: (*b*) data measured using the D10 spectrometer; (*c*) data measured using the TAS6 spectrometer.

The critical behaviour of the magnetization is defined by the equation

$$M = M_0 t^{\beta} \tag{18}$$

where $t = 1 - T/T_C$ and the magnetization is normalized to unity at $T = 0$ K. The critical exponent β and amplitude M_0 were determined from log–log plots, such as those shown in figure 4(*b*) and 4(*c*). The values obtained are listed in table 1. A sharp crossover between two regimes of different exponents β was observed to occur at a reduced temperature of approximately 0.03 (D10 experiment) or 0.015 (TAS6 experiment).

In the asymptotic regime close to T_C, the exponent β was estimated to be 0.33 (TAS6 experiment) or 0.28 (D10 experiment). Both these values are close to the expected 0.31 for the 3D Ising model or 0.33 for the 3D XY model, but significantly different from the value of 0.38 for the 3D Heisenberg model. We discuss the reason for their difference in section 5.4.

Table 1. Summary of results of fits given in figures 4, 5, 7 and 8. The numbers in parentheses are the estimated standard errors.

Figure	Fit to expression	Fitted parameters	Temperature range
4 (TAS6)	$M \sim (52.403 - T)^{\beta}$	$\beta = 0.230(2)$ $\beta = 0.333(19)$	$T < T_C - 0.8$ $T > T_C - 0.8$
4 (D10)	$M = M_0(1 - T/52.225)^{\beta}$	$\beta = 0.224(8)$, $M_0 = 0.96$ $\beta = 0.281(8)$, $M_0 = 1.13$	$T < T_C - 1.6$ $T > T_C - 1.6$
5	$\kappa^2 = \kappa_0^2(T - T_C)^{2\nu} + \kappa_z^2$ (see equation (20))	$\kappa_0^2 = 2.2(2) \times 10^{-5}$ $\kappa_z^2 = 5.3(2) \times 10^{-5}$ $T_C = 52.403(16)$ $\nu = 0.825(25)$	$T > T_C$
7	$\kappa = \kappa_0 \exp(-b/\sqrt{t})$ $t = T/T_{KT} - 1$ (see equation (22))	$\kappa_0 = 0.76(39)$ $b = 2.12(57)$ $T_{KT} = 43.4(2.7)$	$T > 55$ K
8	$\chi = C \exp(B/\sqrt{t})$ $t = T/43.4 - 1$ (see equation (23))	$C = 0.0071$ $B = 4.36(08)$	$T > 55$ K

In the second regime, a well defined exponent $\beta \simeq 0.23$ was observed. As discussed in section 3, this value is characteristic of a finite 2D XY model. The value $\beta = 0.230(2)$ derived from the data measured using TAS6 is in particularly accurate agreement with the theoretical prediction $\beta = 3\pi^2/128 = 0.231\ldots$ [10].

5.2. *Wavevector-dependent susceptibility: $T \geqslant T_C$*

The susceptibility and correlation length data were analysed in three different ways:

(1) via a mean-field formulation of $\chi(q)$;
(2) according to the Kosterlitz expression (7);
(3) according to conventional power-law divergences.

5.2.1. Mean-field analysis. This analysis is only of interest as a method of estimating the weak 3D exchange coupling J'.

Above 55 K the intensity and width of the ridge of diffuse scattering did not exhibit significant periodicity along [0, 0, 1], reflecting the absence of 3D correlations. Below 55 K there was a pronounced modulation with wavevector along [0, 0, 1], with maxima in the intensity and minima in the width at the reciprocal-lattice points (0, 0, 2), (0, 0, 4), etc. This behaviour, which is illustrated in part in figure 2, can be described by a mean-field formulation of the wavevector-dependent susceptibility [23, 30]. For Rb_2CrCl_4, the susceptibility can be written

$$\chi(q) = 4\chi_C/[4(T - T_C)/T_C + a_0^2(q_x^2 + q_y^2) + (J'/J)c_0^2q_z^2] \tag{19}$$

where χ_C is a constant, and q_x, q_y, q_z represent wavevector displacements from a reciprocal-lattice point. If the scattering is fitted to a Lorentzian of half-width κ at half-maximum, then, by analogy with equation (17),

$$\kappa^2 = (\kappa_{MF})^2 + (\kappa_z)^2 \tag{20}$$

where

$$(\kappa_{MF})^2 = (\kappa_0)^2[(T - T_C)/T_C]^{2\nu}$$
$$(\kappa_z)^2 = (J'/J)q_c^2 \tag{21}$$

$\nu = 0.5$, $\kappa_0 = 2$ and $q_c = c_0 q_z$ is the displacement from the Brillouin zone centre along the c direction. The parameters κ, κ_{MF}, κ_0 and q_c are all expressed in reciprocal-lattice units, e.g. $q_c = 0.2$ for $\boldsymbol{Q} = (0, 0, 2.2)$. Equation (19) shows that the measured κ consists of a temperature-dependent part κ_{MF} and a temperature-independent part κ_z arising from the 3D correlations.

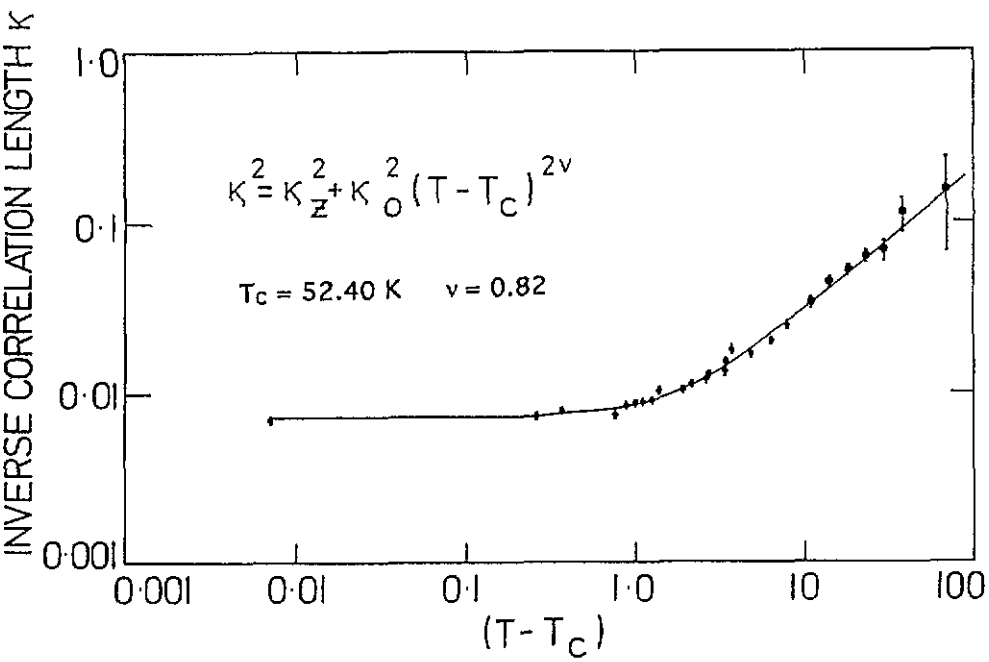

Figure 5. Plot of the fitted Lorentzian width κ measured at $\boldsymbol{Q} = (0, 0, 2.9)$ versus temperature and analysed according to the mean-field approximation equation (20) (see also table 1). The data were measured using the TAS6 spectrometer.

The data were analysed using equations (20) and (21), treating κ_0, κ_z and ν as adjustable parameters, with the results $\nu = 0.82 \pm 0.01$ (TAS6 data; figure 5 and table 1) and $\nu = 0.61 \pm 0.01$ (D10 data), the difference probably arising from the different methods of correcting for the instrumental resolution (see section 5.4). The deviation of ν from the value $\nu = 0.5$ reflects the inaccuracy of the mean-field approximation. For the data obtained using TAS6 ('TAS6 data'), κ_z^2 was found to be 5.3×10^{-5} at $q_c = 0.9$, corresponding to $J'/J \simeq 6.5 \times 10^{-5}$ (see figure 5). Another estimate of J'/J was derived from the data obtained using D10 ('D10 data') at 52.25 K ($\simeq T_C$), by plotting κ^2 versus q_c^2, as shown in figure 6. The result, $J'/J \simeq 1.5 \times 10^{-4}$, is in quite good agreement with the direct estimate of Hutchings *et al* [13] of about 2.4×10^{-4}. A comparison of the data of the two experiments showed that the discrepancy between the two estimates of J'/J arose directly from the different fitted widths κ in the critical region, the D10 estimates being a factor of about 1.5 greater than the TAS6 estimates in this region. The discrepancy was not reflected

in the data at higher temperatures, where the widths were larger, and it was concluded that there was a systematic error in the D10 results near to T_C, arising from the approximate nature of the resolution correction, and possible effects of the more open vertical resolution (see section 4). As argued in section 5.4, the method used—approximating the width of the resolution ellipsoid by the width of a Bragg reflection—would be expected to underestimate the resolution width and to overestimate κ, as observed.

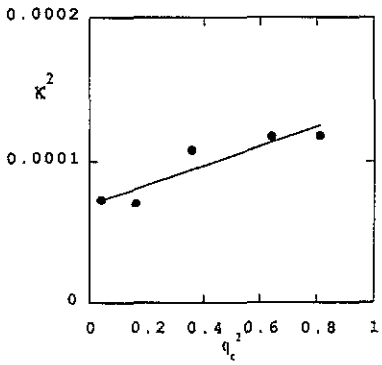

Figure 6. Square of the fitted Lorentzian width κ (measured using the D10 spectrometer) plotted versus the square of q_c (equation (20)). The best-fit line has slope $J'/J = 1.5 \times 10^{-4}$.

5.2.2. Analysis according to the Kosterlitz expression. According to the arguments outlined in section 3, pure 2D XY behaviour is expected to occur at temperatures above the 2D–3D crossover temperature (about 55 K). This corresponds to the paramagnetic regime of the 2D XY model, in which the spin–spin correlations decay exponentially with correlation length ξ (equation (7)). The exact form of $\chi(q)$ is not known with certainty, although the Ornstein–Zernike form (17) is correct for $q < \kappa$ [31], and a good approximation for $q > \kappa$. The susceptibility χ and inverse correlation length κ were therefore obtained from the TAS6 data above 55 K, using equation (17), and then analysed according to the Kosterlitz expression (7).

First, the inverse correlation length was fitted using least-squares minimization to the equation

$$\kappa = \kappa_0 \exp(-bt^{-1/2}) \tag{22}$$

where $t = T/T_{KT} - 1$, by varying the parameters κ_0, b and T_{KT}. As shown in figure 7, equation (22) is found to fit the data very accurately indeed, with the result $\kappa_0 = 0.76 \pm 0.39$, $b = 2.12 \pm 0.57$ and $T_{KT} = 43.4 \pm 2.7$ K. These values are remarkably close to those expected theoretically; the amplitude κ_0 is of order unity, and the value of $b = 2.1$ is very close to the corrected prediction of Kosterlitz of 1.9 and the best Monte Carlo estimate of Gupta *et al* [17] of 1.8. These results are summarized in table 1 and discussed further in section 6.

The susceptibility χ of the 2D XY model may be derived from the scaling law $\chi \simeq \xi^{2-\eta}$, with the result [14]

$$\chi = C \exp(Bt^{-1/2}) \tag{23}$$

where $B = (2 - \eta)b$ and C is a constant, which in the present context is simply a normalization factor, with no physical meaning. The experimentally derived susceptibility $\chi(0)$ was fitted to (23), using $T_{KT} = 43.4$, derived as described above from the temperature variation in the inverse correlation length. It was found that $B = 4.36 \pm 0.08$. Treating T_{KT}

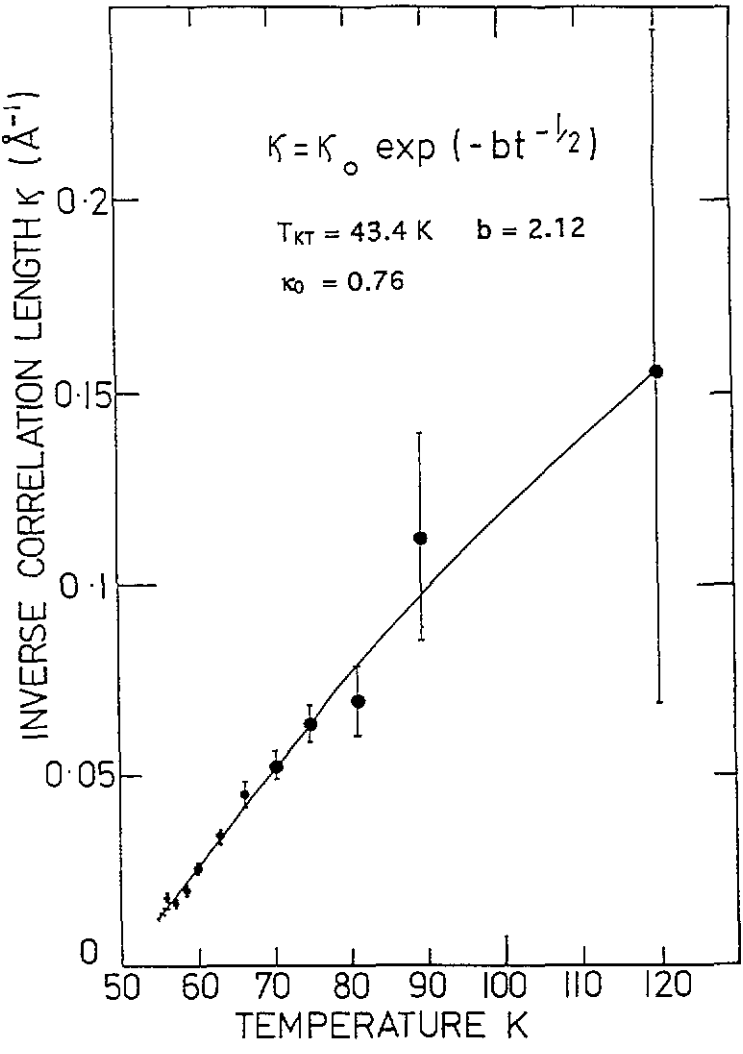

Figure 7. Temperature dependence of κ, the inverse correlation length measured in the 2D regime, measured using the TAS6 spectrometer, fitted to the Kosterlitz expression (22) (see also table 1).

as an adjustable parameter gave $T_{KT} = 43.9$ K and $B = 4.18 \pm 0.66$. These results are in excellent agreement with the results of Cornelius *et al* [9], who found that $B = 4.07 \pm 0.10$ from magnetization measurements on Rb_2CrCl_4. B is also very close to the value expected from the results of the fits to the correlation length; with $b = 2.12$ and taking $\eta \simeq 0$, we find that $B = 4.24$. An example of a fit to the susceptibility data is illustrated in figure 8, and the results are listed in table 1.

Attempts to estimate the exponent η from the susceptibility data indicated that $\eta \simeq 0$, but the errors were very large (± 0.3). For the 2D XY model, $\eta = 0.25$ at T_{KT}, but the behaviour of η in the paramagnetic regime is not well established [31]. If one assumes that $\eta \neq 0$ in the paramagnetic regime, then η can be estimated by using, rather than the Lorentzian form (11), the expression

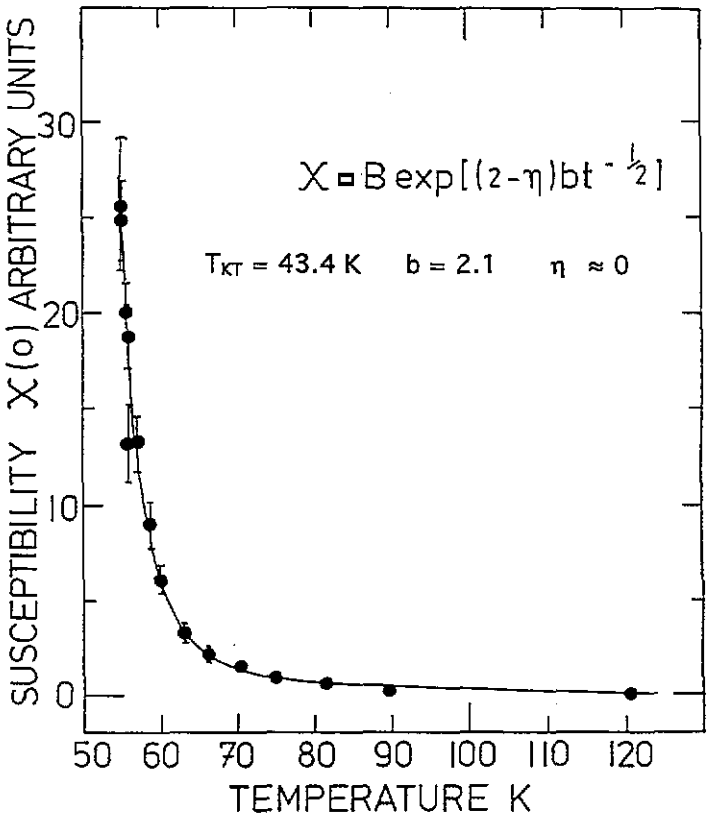

Figure 8. Temperature dependence of the susceptibility $\chi(0)$ measured in the 2D regime, using the TAS6 spectrometer, fitted to the Kosterlitz expression (23) (see also table 1). Note that the figure shows the fit for the amplitude B held equal to 4.2 ($= 2b$; see text).

$$\chi(q) \simeq 1/(q^2 + \kappa^2)^{1-\eta/2}. \tag{24}$$

However, we found no significant deviation from a Lorentzian function.

Finally, in another experiment, which we do not report in detail here, we determined the susceptibility by integration over energy transfer of the inelastic neutron scattering spectrum, measured on the IN12 spectrometer at the ILL, Grenoble. The temperature dependence of $T\chi(q = 0)$ was found to be in almost exact agreement with the result obtained using TAS6, confirming both the validity of the quasi-static approximation, and the method of analysis of the data.

5.2.3. Analysis according to conventional power laws. For completeness, the correlation length and susceptibility measured using TAS6 were also fitted to the conventional power laws [25]

$$\begin{aligned} \chi T &\propto (1 - T_C/T)^{-\gamma} \\ \kappa &\propto (T/T_C - 1)^{\nu}. \end{aligned} \tag{25}$$

Fitting the data in the 2D regime above 55 K gave the results $\gamma = 2.5 \pm 0.07$ K and $\nu = 1.06 \pm 0.17$ K (see table 1). These critical exponents are not characteristic of any known universality class.

Since the fits of the data to conventional power laws and to the KT theory are equally accurate, any judgment between the relative merits of the two approaches must rely on the parameters obtained in the fits. We therefore favour the KT theory on the grounds of self-consistency, since all the derived parameters are in excellent agreement with theoretical predictions, and with the conclusions of other experiments. It is probable that the critical exponents γ and ν are simply fitting parameters, with no physical meaning.

5.3. Wavevector-dependent susceptibility: $T \leqslant T_C$

The wavevector-dependent susceptibility was observed to maintain its approximately Lorentzian form below T_C, with κ initially increasing slightly with decreasing temperature. As shown in figure 9, κ became only weakly temperature dependent below about 51 K, which corresponds to the 2D regime of the magnetization (see section 5.1). The modulation of the width with q_c due to the 3D coupling J' (equation (19)) was also observed to be independent of temperature in this regime (figure 9). The extrapolated value of κ at $q_c = 0$ was estimated from the D10 data to be about $0.0125/a_0$, corresponding to a correlation length of about 80 lattice spacings. However, as explained in section 5.2.1 above, the correlation length estimated from the D10 data was inaccurate by a factor of approximately 1.5 in this region, and so a more accurate estimate is about 120 lattice spacings. The results presented in figure 9 are nevertheless expected to be qualitatively correct.

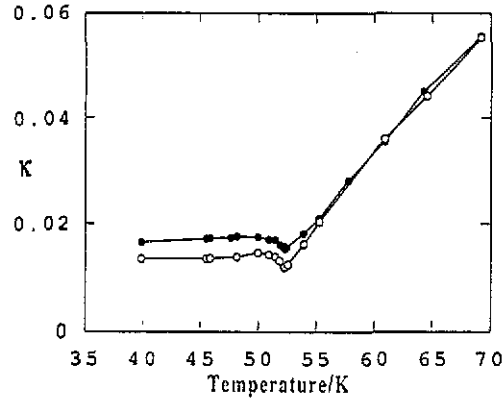

Figure 9. Fitted width κ of the [0,0,1] diffuse rod measured at $Q = (0, 0, 2.4)$ (○) and $Q = (0, 0, 2.8)$(●), near and below T_C. The data were measured with the D10 spectrometer. Note that the fitted values of κ are a factor of about 1.5 larger than those derived from the data measured with the TAS6 spectrometer, probably as a result of the approximate resolution function used in the fitting procedure (see section 5.2.1).

5.4. Comparison of the results of the two experiments

The two experiments yielded results in qualitative agreement, but with some quantitative differences. Firstly, the value of the three-dimensional ordering temperature T_C was found to be slightly lower in the experiment performed on D10 (52.225 K) than in that performed on TAS6 (52.403 K). This probably reflected the difference between the two samples. That measured on D10 was an older sample at the time of the experiment and so may have been less pure; Rb_2CrCl_4 samples are susceptible to oxidation, even when handled with care.

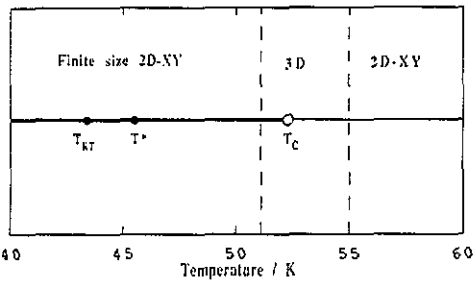

Figure 10. Phase diagram of the critical region of Rb_2CrCl_4 in zero magnetic field, indicating regions of universal behaviour: ——, region of spontaneous order; ●, ⊙, experimentally determined temperatures T_{KT}, T^* and T_C, referred to in the text.

Impurities would generally give a lower transition temperature. The lower 3D magnetization exponent measured on D10, $\beta = 0.28$, could also be explained by the presence of impurities. That measured on TAS6, $\beta = 0.33$, is closer to the expected value for 3D ordering.

A more serious discrepancy between the two sets of results was the quantitative differences in the measured correlation length. This certainly resulted from the different methods of correcting for instrumental resolution (see section 5.3). The method used to treat the data collected on D10 involved convolution of the scattering function with a fixed 'resolution width'. The latter was derived from the width of nearby Bragg peaks, a method which underestimates the resolution width, since it measures a diameter of the resolution ellipsoid rather than its projection on the scan direction. The method also neglects the finite vertical resolution of D10, which was used without vertical collimation. An approximate correction for these errors brought the measured correlation length to a value consistent with that obtained on TAS6, where the correction for both horizontal and vertical instrumental resolution was performed rigorously within the theoretical description of Cooper and Nathans [32].

Overall, we expect the results of the experiment performed on TAS6 to be the more accurate. This is confirmed by their very close agreement with the theoretical predictions.

6. Discussion

In general the behaviour of Rb_2CrCl_4 confirms the expected crossover behaviour described in the introduction and in section 3. The asymptotic critical behaviour is 3D, but there are crossovers to 2D XY-like behaviour both above and below T_C.

The experimental T_{KT} (see table 1) of 43.3 K corresponds to a value of about 0.71 in units of $2JS^2$. This may be compared to the prediction of 0.898 for the classical 2D XY model (see section 3). This difference is not surprising, since the out-of-plane fluctuations in Rb_2CrCl_4 would be expected to reduce the absolute value of the transition temperature.

It is now possible to check the detailed predictions for the finite-sized XY behaviour of the ordered phase, described in section 3. We first identify the effective system size L_{eff}. This is a parameter of the order $\sqrt{J/J'}$ but is not necessarily equal to $\sqrt{J/J'}$. Probably the best estimate is the value of the correlation length in the 2D XY regime, which is approximately 120 lattice spacings (see above). This is equal to the mean-field estimate of $\sqrt{J/J'}$ (see figure 5) and is of the order of the more accurate spin-wave estimate of about 60.

The temperature at which $\delta = 15$ and $\eta = 0.25$, which we now understand to be T^*, was previously identified by Cornelius *et al* [9] to be 45.5 K. At T^*, the observed magnetization $M(T)/M(0)$ is predicted to be approximately $(1/L_{\text{eff}}\sqrt{2})^{1/8} \simeq 0.55 \pm 0.02$ (see equation (10)). The observed value (figure 4) is 0.6 ± 0.02, in quite good agreement. One should perhaps not expect a better agreement between the XY model and Rb_2CrCl_4 as regards the *magnitude* of the magnetization. However, in accord with universality, the subcritical exponent β at T^*, defined relative to $T_C = 52.403$ K, is found to be 0.230(2), in extremely accurate agreement with the theoretical prediction $3\pi^2/128 = 0.231\ldots$.

In order to make a more detailed test of the predictions of section 3, we use equations (11) and (13), and the estimates derived from the behaviour of the correlation length: $T_{KT} = 43.3$ K, $b = 2.12$ and $L_{\text{eff}} = 120$. This gives $T^* \simeq 45.4$ K and $T_C \simeq 52.8$ K. These are, within the error to which they can be estimated, equal to the observed $T^* = 45.5$ K, and the 3D ordering temperature $T_{3D} = 52.4$ K, respectively. As mentioned in section 3, there is no reason why T_C and T_{3D} should be identical. The fact that they are very close ensures that $\beta = 0.23$ is easily observed experimentally.

The excellent agreement between theory and experiment, confirms that Rb_2CrCl_4 behaves like a finite-sized 2D XY system in the 2D subcritical regime both below and above T_C. This suggests that spin vortices exist in Rb_2CrCl_4, since the theory of Kosterlitz [14], as modified for a finite system [10], assumes their existence, and they are observed in Monte Carlo simulations. However, unbound vortices probably occur only in large numbers at $T > T^*$ [33].

It is perhaps surprising that the temperature dependence of the 3D magnetization should be determined by 2D fluctuations over a wide temperature range. This may be understood as follows. Below T_C, in the 3D ordered phase, the correlation length decreases until it becomes of order $\sqrt{J/J'}$, at the 2D–3D crossover temperature. At lower temperatures, the temperature dependence of the magnetization of each layer is determined by misaligned regions of all sizes up to this correlation length. These regions are in general too small to be correlated with those in neighbouring layers. Thus, while the magnetization of each layer is strongly correlated in 3D, the fluctuations in the magnetization are only weakly correlated. The system therefore behaves as an assembly of layers connected in a mean-field manner, and one measures a 3D magnetization which varies in the manner of a finite 2D system.

It is interesting to observe that the staggered twofold in-plane anisotropy, which approximates to a fourfold bulk anisotropy, is irrelevant in determining the 2D critical properties. José *et al* [15] predicted that a fourfold field h_4 was only marginally relevant, with non-universal critical exponents. One would therefore expect h_4 to manifest itself only very close to T_C, and it is clear that for Rb_2CrCl_4 this does not occur in the 2D regime. It is, however, likely that h_4 becomes important in the 3D regime, probably resulting in Ising-like behaviour. The experiments are consistent with this.

In figure 10 we summarize the crossover behaviour of Rb_2CrCl_4 on a phase diagram. Omitted from the diagram are the 2D Heisenberg regime (which is observed well above T_C) and the low-temperature spin-wave regime [3] (which is non-universal).

7. Summary and conclusions

The critical behaviour of Rb_2CrCl_4 reflects the presence in the Hamiltonian of several terms of differing orders of magnitude. The dominant behaviour is 2D XY like, with crossover to 3D XY or 3D Ising-like behaviour occurring near to T_C.

In the 2D regime below T_C, the behaviour of the magnetization was found to be in excellent quantitative agreement with theoretical predictions [10] for a finite 2D XY model.

The in-plane correlation length is found to be only weakly temperature dependent, with the approximate value of $\sqrt{J/J'}$ lattice units.

In the 2D regime above T_C, the behaviour of the correlation length was found to be in excellent quantitative agreement with the prediction of Kosterlitz [14] and Monte Carlo simulations [17] for the 2D XY model. In this regime there is no need to distinguish between the finite and infinite systems, because the behaviours are the same.

The effective fourfold anisotropy of Rb_2CrCl_4 appears to have no effect on the critical properties in either 2D critical regime, consistent with the predictions of José *et al* [15].

In general, we have found excellent agreement between experiment and theory. Our principal conclusion is that the RG equations of José *et al* [15] and Kosterlitz [14], when modified for finite-size effects [10], describe all the essential physics of the magnetism of Rb_2CrCl_4 in the subcritical regime.

Acknowledgments

We would like to thank K R A Ziebeck for experimental assistance, I Osborn for help with the data analysis and P C W Holdsworth, M Thorpe and P Day for very useful discussions. MTH would also like to thank Risø National Laboratory for their hospitality during his visit. This work was supported in part by the Underlying Research Programme of the UKAEA, and by the SERC.

References

[1] Janke E, Hutchings M T, Day P and Walker P J 1983 *J. Phys. C: Solid State Phys.* **16** 5959
Day P, Fyne P J, Hellner E, Hutchings M T, Münninghoff G and Tasset F 1986 *Proc. R. Soc.* A **406** 39
[2] Fair M J, Gregson A K, Day P and Hutchings M T 1977 *Physica* B **86–88** 657
[3] Hutchings M T, Als-Nielsen J, Lindgard P A and Walker P J 1981 *J. Phys. C: Solid State Phys.* **14** 5327
[4] Collins M F 1989 *Magnetic Critical Scattering* (Oxford: Oxford University Press)
[5] Mermin N D and Wagner H 1966 *Phys. Rev. Lett.* **17** 1133
[6] Kawabata C and Bishop A R 1986 *Solid State Commun.* **60** 167
[7] Kosterlitz J M and Thouless D J 1973 *J. Phys. C: Solid State Phys.* **6** 1181
[8] Berezinskii V L 1971 *Sov. Phys.–JETP* **32** 493
[9] Cornelius C A, Day P, Fyne P J, Hutchings M T and Walker P J 1986 *J. Phys. C: Solid State Phys.* **19** 909
[10] Bramwell S T and Holdsworth P C W 1993 *J. Phys.: Condens. Matter* **5** L53
Bramwell S T and Holdsworth P C W 1993 *J. Appl. Phys.* **73** 6096
[11] Harrop M C 1981 *D.Phil Thesis* University of Oxford
[12] Elliot R J, Hengeltraub A, Harrop M C and Ziman T A L 1980 *J. Magn. Magn. Mater.* **15–8** 359
[13] Hutchings M T, Day P and Fyne P J 1984 unpublished results
Fyne P J 1984 *DPhil Thesis* University of Oxford
[14] Kosterlitz J M 1974 *J. Phys. C: Solid State Phys.* **7** 1046
[15] José J V, Kadanoff L P, Kirkpatrick S and Nelson D R 1977 *Phys. Rev.* B **16** 1217
[16] Villain J 1975 *J. Physique* **36** 581
[17] Gupta R, DeLapp J, Batrouni G C, Fox G C , Baillie C F and Apostolakis J 1988 *Phys. Rev. Lett.* **61** 1996
[18] Bramwell S T and Holdsworth P C W 1993 submitted for publication
[19] Berezinskii V L and Blank A Ya 1973 *Sov. Phys.–JETP* **37** 369
[20] Nelson D R and Kosterlitz J M 1977 *Phys. Rev. Lett.* **39** 1201
[21] Hirakawa K and Ikeda H 1973 *J. Phys. Soc. Japan* **35** 1328
[22] Regnault L P and Rossat-Mignod J 1990 *Magnetic Properties of Layered Transition Metal Compounds* ed L J de Jongh (Deventer: Kluwer)
[23] Marshall W and Lowde R D 1968 *Rep. Prog. Phys.* **31** 705
[24] Als-Nielsen J 1976 *Phase Transitions and Critical Phenomena* vol 5a, ed C Domb and M S Green (New York: Academic)

[25] Stanley H E 1971 *Introduction to Phase Transitions and Critical Phenomena* (reprint 1987) (Oxford: Oxford University Press)
[26] Birgeneau R J, Guggenheim H J and Shirane G 1970 *Phys. Rev.* B **1** 2211
[27] Hutchings M T, Day P, Janke E and Pynn R 1896 *J. Magn. Magn. Mater.* **54–7** 673
[28] Garton G and Walker P J 1976 *J. Cryst. Growth* **36** 351–2
[29] Hutchings M T, Lowde R D and Tindle G L 1986 *Workshop on Neutron Scattering Data Analysis (Inst. Phys. Cont. Ser. 8)* (Bristol: Institute of Physics) p 151
[30] Hirakawa K 1982 *J. Appl. Phys.* **53** 1983
[31] Heinkamp S W and Pelcovits R A 1985 *Phys. Rev.* B **32** 4528
[32] Cooper M J and Nathans R 1967 *Acta Crystallogr.* **23** 357
[33] Weber H and Jensen H J 1991 *Phys. Rev.* B **44** 454